VOL. 13, NO. 24, DECEMBER 2018 ISSN 1819-6608
ARPN Journal of Engineering and Applied Sciences

www.arpnjournals.com

CHARACTERIZATION AND ELECTRICAL CONDUCTIVITY OF IONIC OXIDE NANO FILMS BY DC AND AC METHODS

S. N. Padhi[1], K. S. Raghu Ram[2], A. Sai Neel Kamal[2], Ch. Siva Rama Krishna[2] and B. N. Dhanunjaya Rao[2]
[1]Koneru Lakshmaiah deemed to be University Vijayawada, India
[2]Vignan's Institute of Information Technology, Visakhapatnam, India
E-Mail: snpadhi@kluniversity.in

ABSTRACT

We report here the ionic conductivity characteristics of single crystal of Yttria Stabilized Zirconia (YSZ)<100>. The targets of YSZ of one-inch diameter and about 2-3 mm thickness were palletized and sintered in the range of 1000-15000 C for 2-4 hours in air. These targets were polished up to 1000 emery paper cleaned in an ultrasonic bath containing methanol. The ionic conductivity was measured using both AC impedance spectroscopy and DC four probe technique. An idealized plot for the spectrum of a ceramic oxide specimen with particularly blocking electrodes has been studied. The ionic conductivity of ceramic oxide was compared with YSZ <100>.The investigation showed that the advantage of AC method is to separate the bulk, grain boundary and electrode resistance which is not possible by DC method. A single crystal of YSZ<100> was experimented for ionic conductivity. The ionic conductivity and activation energy of YSZ<100> at 973 K were found to be almost same in both DC and AC method which seems to be because of absence of grain boundary.

Keywords: ionic conductivity, grain boundary, activation energic method, impedance spectroscopy, D.C method.

INTRODUCTION

Ionic conductors have provided a fascinating interdisciplinary field of study ever since their discovery by Faraday at the Royal Institution in London over 200 years ago [1]. More recently, and particularly in the past decade, the place of research has been rapid, driven by the requirements for new clean energy sources, sensors, and high energy density batteries. A very interesting subgroup of this class of materials is the oxides that display oxygen ionic conductivity. There has been a continued drive for their development because of the promising impact of the technological devices such as the solid oxide fuel cell (SOFC), oxygen separation membranes, opto -electronic devices and many more. These devices offer the potential of enormous commercial and ecological benefits provided suitable high -performance materials can be developed. The search for novel materials with enhanced ionic conductivity for application in energy devices has uncovered an exciting new facet of oxide interfaces.

With judicious choice of the constituent materials, oxide heterostructures can exhibit enhanced ion mobility compared to the bulk counterparts [12]. Oxide -based ionic conductors have attracted tremendous research interests due to their wide applications in energy storage and conversion devices, such as photo voltaics, fuel cells, batteries, and super capacitors. Extensive efforts have been undertaken to improve the ionic conductivity of existing materials along with the development of novel conductors [13].

Super ionic materials are necessarily the oxides, which have high ionic conductivity at intermediate operating temperatures. High ionic conductivity results due to defect formation by doping a lio valent guest cations to the host compounds which replace partly the host cations and create vacancies in the oxygen sites for charge neutrality. These vacancies provide a conduction path for the oxygen ions to carry the charge thereby increasing the ionic conductivity. YSZ as the electrolyte of choice has dominated the progressive development of solid oxide fuel cell (SOFC) technologies for many years. To enable SOFCs operating at intermediate temperatures of 600 °C or below, major technical advances were built on a foundation of a thin-film YSZ electrolyte [14].

Experimental techniques

The targets of YSZ of 1inch diameter and about 2-3 mm thickness were palletized and sintered in the range 1000 -1500 ^{o}C for 2-4 hours in air. These targets were polished up to 1000 emery paper, cleaned in an ultrasonic bath-containing methanol. The ionic conductivity was measured using both AC impedance spectroscopy and DC Four Probe technique. The electrical conductivity in ionic conductors is generally dominated by ions although both ions as well as electrons conduct current. Under the applied electric field, the total resistance offered by the material and the electrodes is

$$R_{tot} = \frac{R_b}{[R_{gb} + R_{el}]}$$

Where Rtot, Rb, Rgb and Rel are the resistances of total, bulk, grain boundary and electrodes respectively. DC-four probe method: When a sample is mounted between two inert electrodes, DC measurements cannot be performed directly owing to polarization of the electrodes. This polarization phenomenon can be avoided by making use of a method with four electrodes (Figure-1). A constant current is applied by a DC current calibrator between two outer electrodes and by measuring the voltage drop by microvoltmeter between the two inner electrodes, the electrical conductivity is calculated. Since no current flows in the inner two electrodes, neither

polarization effects, nor contact resistances occur at the inner electrodes.

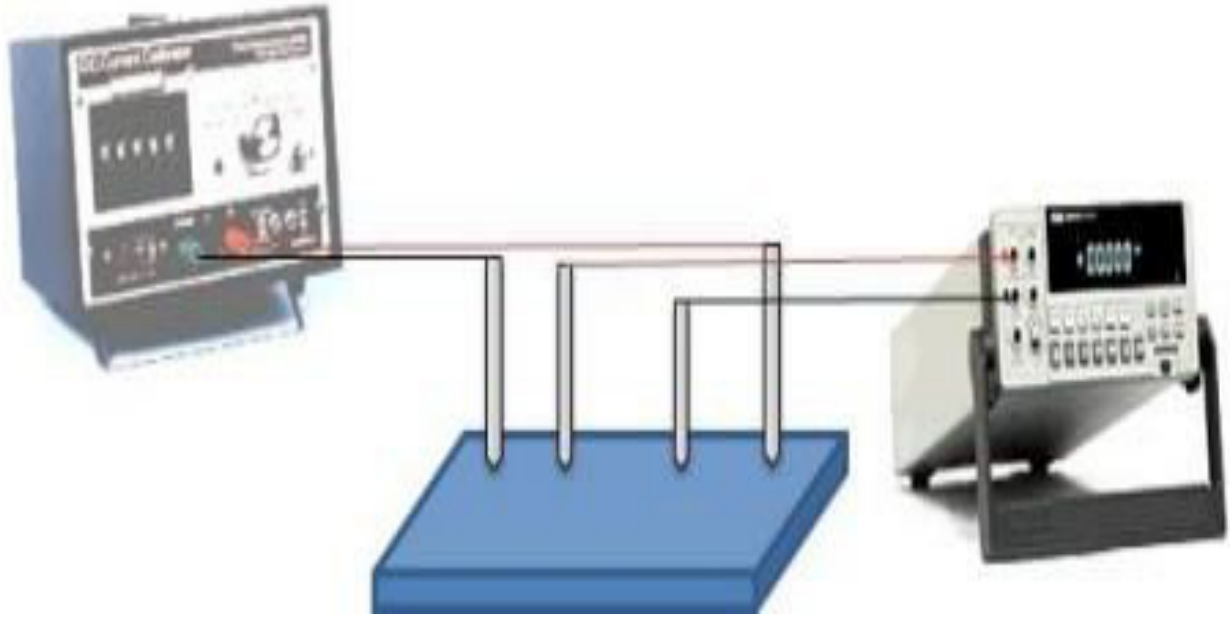

Figure-l. Schematic of four point probe technique for conductivity experiments.

AC-impedance spectroscopy

Historically the electrical conductivity have been measured by DC-four probe method on sintered ceramic samples. This can lead to errors because of effects due to the behavior of grain boundaries and electrodes, which may mask the true behavior of the bulk. This uncertainty can be removed by use of the complex plane impedance analysis first applied to solid electrolytes by Bauerle (1969). In this method the complex impedance Z or equivalently, the complex admittance Y (Z=I / Y) of a specimen is plotted on an Argand diagram for a large range of frequencies, usually from 1 Hz to 105 Hz. An idealized plot for the spectrum of a ceramic oxide specimen with particularly blocking electrodes is shown in Figure-2 below. The spectrum consists of three semicircles which may be tilted below the real axis by differing amounts. The number of semicircles seen depends upon, the temperature range and frequency range used. The frequency is varied using an impedance/gain phase analyzer.

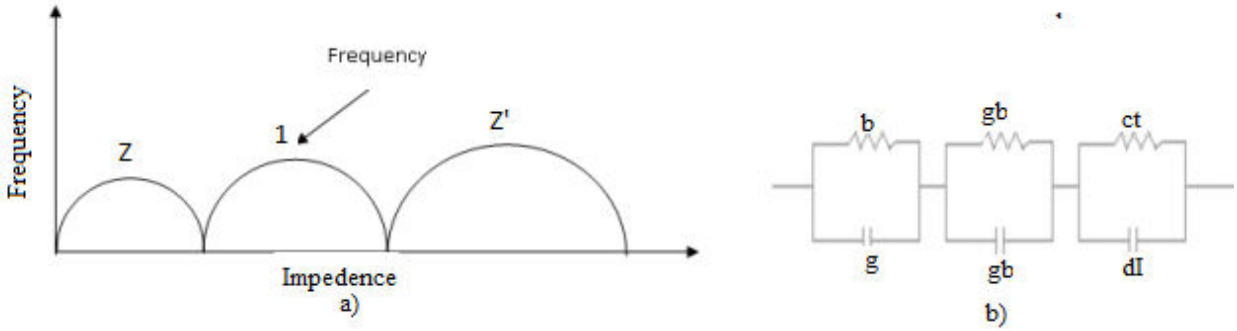

Figure-2. (a)An idealized complex impedance plot for a ceramic oxide with partially blocking electrodes, (b) An equivalent circuit representing the ceramic specimen corresponding to (a).

The conductivity of semiconducting materials is known to be frequency dependent, which as expected is due to conduction in the localized state. Since the charge carriers are localized, ac technique is a powerful experimental method often employed to probe their behavior [2-4]. The ac conductivity $\sigma_{ac}(\omega)$, of amorphous semiconductors is usually expressed as

$$\sigma_{ac}(\omega) = \sigma_T - \sigma_{dc} = A\omega^S$$

where ω is the angular frequency of the applied field, A is a constant, S($\leq$ 1.0) is frequency exponent, σ_T is the total conductivity including the frequency dependent conductivity under ac field and σ_{dc} is the dc conductivity [5-10]. The influence of the interfaces on the conduction properties of heterostructures is becoming increasingly important with the miniaturization of solid -state devices, which leads to an enhanced interface density at the expense of the bulk [11]. This type of plot is generally

analyzed by the example of Bauerle (1969) who assigned an equivalent circuit to the specimen consisting of lumped RC elements, Each RC element gives rise to a semicircle with a particular time constant or relaxation time.

The semicircles will be well defined provided their relaxation times are well separated. The tilting ofthe relaxation semicircles is usually taken as an indication of the spread of the values of the elementscontributing to a lumped circuit unit. An equivalent circuit for a ceramic oxide corresponding to the impedance plot in Figure-2(a) is shown inthe Figure-2(b). Schouler *et al*. (1973) have pointed out that these equivalent circuits are not unique. however, they also have many of the same general characteristics. The electrodes are taken tobe partially blocking and are represented in the equivalent circuit by Cdl, the double layer capacitance, and Rct, the charge transfer resistance. A bulk resistance, R_b, in parallel with a geometric capacitanceCg, represents the behaviour of the grains of the ceramics. The grain boundaries can be a littlemore complicated because they represent a component both in parallel and in series with the grains.Normally the boundary resistance is much higher than that of the grains and only the seriescontribution need be considered. This resistance is a shunted capacitance C_{gb}. The electricalbehavior of the ceramic sample can therefore be represented in a very simple manner by theseries of RC circuit.

The relative values of the RC units for each component determine the frequency range of the semicircle.For ceramic oxides, the low frequency semicircle is due to electrode dispersion , the intermediate frequency circle is due to the grain boundaries , and the high frequency semicircle is due to thebulk beiavior . The intercepts on the real axis of Figure-2(a) R_1, R_2, and R_3 can be related to the equivalentcircuit as

R_1 —> R_b,

R2 – Rb + Rgb,

R3 = R2 + Rct

It is therefore theoretically possible, by using complex plane impedance analysis, to separate bulk and grain boundary resistances in a sample in a simple arid elegant manner.

RESULTS ANIL DISCUSSIONS

DC four probe method

The conductivity of YSZ <100> single crystal of size 10 x 10 x 0.5 mm was measured using DC technique since single crystals eliminate the contribution of grain boundary resistance in the bulk behavior even at lower temperature. Supplying a constant current of few µA each time, voltage was read from the micro -voltmeter at different intervals of temperature between 523 and 973 K. The resistance obtained from the current and voltage was used to find out the resistivity and thus the conductivity. Resistivity was found from the resistance and cross-sectional dimension of the sample using the relation:

$$R = \rho \frac{l}{A}$$

Where R,ρ,L and A are the resistance , resistivity, length between the voltage carrying probes and area of the sample respectively.

A typical plot between logarithmic conductivity and temperature of YSZ <100> single crystal is shown below. The temperature dependence of conductivity is given by the Arrhenius equation

$$\sigma = \sigma_0 \exp \wedge (Ea/Kt)$$

$$\ln \sigma = \ln \sigma_0 + [-E_a/K] * [1/T]$$

Where σ and σ_0 are the electrical conductivity and pre-exponential factor respectively. E_a, K and T are the activation energy, Boltzmann `s constant and temperature respectively. The above equation ends up with a straight line between ln σ and T, the slope of which is [E_a/K]. Using this, the activation energy of YSZ <100 > was found out to be 0.681 eV (Figure-3); these values are slightly below the reported values of 0.8 and 0.9. The lower activation energy implies an easier ionic motion. This might be due to the absence of grain boundary resistance. The conductivity at 1173 K was found to be 0.159S/cm which is slightly higher than the conductivity of YSZ poly crystals as reported. This may again be accounted for the low contribution of grain boundary resistance.

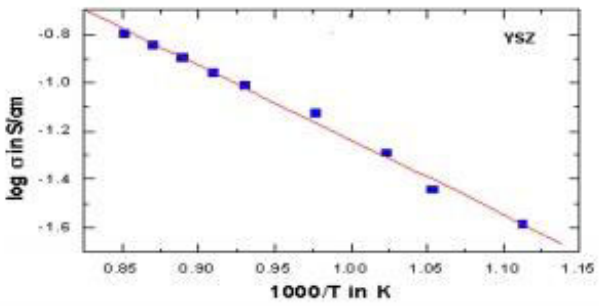

Figure-3. Effect of temperature on conductivity of bulk <100>YSZ single crystal.

AC Impedance method

The conductivities of YSZ <100 > was measured by AC -impedance spectroscopy by supplying a voltage of 50 mV to the sample at frequencies ranging from 32 MHz to 0.01 Hz. Decreasing frequency was found to have a pronounced effect on the phase difference between current and voltage. The phase difference approaches almost to zero when the frequency is decreased from 32 MHz to 0.01 Hz. The response of impedance of the sample in terms of real and imaginary part was found to be semicircular which showed that the samples are not purely ionic but some amount of electronic conductivity is associated. The presence of this electronic conductivity appeared to have taken the semicircular arcaway from the

origin of the plot as shown below, however increasing temperature decreases the electronic conductivity contribution and thus the semicircular arc being away from the origin. The typical arcs found from the instrument are shown below for the YSZ <100> single crystal.

The conductivity of YSZ <100> by AC-impedance method at 1123 K was found to be 0.07 S/cm. The activation energy calculated using the above equation was found to be 0.835 eV (Figure-4).

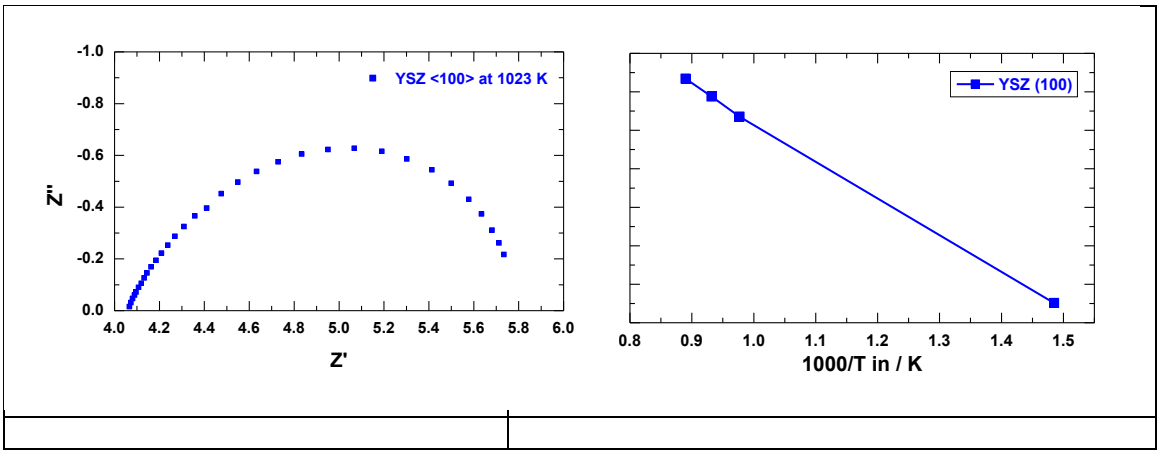

Figure-4. (a) Complex impedance plot between imaginary impedance (Z'') and real impedance (Z') of YSZ <100> single crystal at 1023 K and (b) Conductivity versus inverse temperature plot.

CONCLUSIONS

The ionic conductivity measurement, both by DC four probe and AC impedance spectroscopy has been discussed. The advantage of AC method is to separate the bulk, grain boundary and electrode resistance which is not possible by DC method. A single crystal of YSZ <100 > was experimented for ionic conductivity. The ionic conductivity and activation energy of YSZ<100> at 973 K were found to be almost same in both DC and AC methods which seems to be because of absence of grain boundary.

ACKNOWLEDGEMENT

We are thankful to DOE and Institute of Physics for their kind cooperation and encouragement.

REFERENCES

[1] H.lnaba, H.Tagawa. 1996. Solid State lonics. 83: 1-295.

[2] A. N. Sreeram, A. K. Yarshneya, D. R. Swiler. 19991. J. Non-Cryst. Solids. 130, 225.

[3] A. Rahman, P. C. Mahanta. 1979. Thin Solid Films. 66, 125.

[4] S. P. Fu, Y. F. Chen. 2003. J. Appl. Phys. 93, 2140.

[5] M. 1. Mohammed, A. S. Abd-rabo, E. A, Mahmoud. 2002. Egypt. J. Sol. 25, 49.

[6] S. R. Elliott. 1987. Advances in Physics. 36, 135.

[7] j M. Fadel, S. S. Fouad. 2001. J. Materials Science. 36, 3667.

[8] M. M. EI-Nahass, H.M. Zeyada. M.M. EI-Samanoudy, E. M. El-Menyawy. 2006. J. Phys. Condens . Mater 18 5163.

[9] A. K. Jonscher. 1977. Nature. 267, 673.

[10] N. Mehta, D. Kumar, S. Kumar, A. Kumar. 2005. Chalcogenide Lett. 2, 103.

[11] F.Emiliana, P.Daniele and T.Enrico. 2010. Science and Technology of Advanced Materials. 11, 5.

[12] L.Carlos, S.Jacobo and B.Bernard A. 2013. Functional Oxide Interfaces. 38, 12.

[13] W.Tao *et al.* 2016. Critical Reviews in Solid State and Materials Sciences. 43, 1.

[14] C.Yixiao *et al*. 2018. Journal of Power Sources. 384, 30.